

The Tensor Pomeron and Small-x Deep Inelastic Scattering

Daniel Britzger

Max-Planck-Institut für Physik, Föhringer Ring 6, D-80805 München, Germany

E-mail: britzger@mpp.mpg.de

Carlo Ewerz*

Institut für Theoretische Physik, Universität Heidelberg,

Philosophenweg 16, D-69120 Heidelberg, Germany

and

ExtreMe Matter Institute EMMI, GSI Helmholtzzentrum für Schwerionenforschung,

Planckstraße 1, D-64291 Darmstadt, Germany

E-mail: C.Ewerz@thphys.uni-heidelberg.de

Sasha Glazov, Stefan Schmitt

Deutsches Elektronen-Synchrotron DESY, Notkestraße 85, D-22607 Hamburg, Germany

E-mail: Alexandre.Glazov@desy.de, Stefan.Schmitt@desy.de

Otto Nachtmann

Institut für Theoretische Physik, Universität Heidelberg,

Philosophenweg 16, D-69120 Heidelberg, Germany

E-mail: O.Nachtmann@thphys.uni-heidelberg.de

We apply the tensor-pomeron model to small- x deep-inelastic lepton-proton scattering and photoproduction. Our model includes a soft and a hard tensor pomeron as well as a reggeon contribution. Data with c. m. energies $6 < \sqrt{s} < 318$ GeV and virtualities $Q^2 < 50 \text{ GeV}^2$ are considered. Our fit gives a very good description of the available data in this kinematic region, including the latest HERA data for $x < 0.01$. In particular, the transition region from low to high Q^2 is well described. Within the errors, the hard pomeron is absent in photoproduction. The intercepts of the soft and hard pomeron in the two-tensor-pomeron model are found to be $1.0935^{(+76)}_{(-64)}$ and $1.3008^{(+73)}_{(-84)}$, respectively. We argue that a vector pomeron would not give any contribution to photoproduction.

XXVII International Workshop on Deep-Inelastic Scattering and Related Subjects - DIS2019

8-12 April, 2019

Torino, Italy

*Speaker.

1. Tensor pomeron

High energy hadronic reactions are dominated by the physics of the pomeron. For example, total cross sections, related to the elastic forward scattering amplitude by the optical theorem, are at high c. m. energy described by the exchange of a pomeron in the t -channel. For soft reactions, calculations of the pomeron from first principle are currently not possible, and one has to retreat to Regge models to describe soft high-energy scattering. Here, we want to discuss deep inelastic scattering (DIS) in the context of such a Regge model. This presentation summarizes some of the key results of [1] to which we refer the reader for further details.

Until recently, the spin structure of the pomeron has not received much attention. It is well known that the pomeron carries vacuum quantum numbers with regard to charge, color, isospin and charge conjugation. But what about spin? It has been shown some time ago that the pomeron can be regarded as a coherent superposition of exchanges with spins 2, 4, 6, etc [2]. The new aspect that we want to discuss here is the structure of the couplings of the pomeron to external particles. Most models treat these couplings like those of a photon [3], i. e., as vector couplings. In many fits to DIS data the coupling is not specified at all and only the energy dependence of the pomeron enters the formulae used for fitting the data, see for example [4]. We argue that the pomeron couplings play an important role, and that they should be treated as tensor couplings. Two of us, in collaboration with M. Maniatis, have constructed an effective theory with such a tensor pomeron and reggeon contributions (and a vector odderon) [5].

Conceptually, vector-type couplings of the pomeron turn out to be rather questionable. For example, a vector pomeron implies that the total cross sections for pp and $\bar{p}p$ scattering at high energy have opposite sign. But, of course, quantum field theory forbids negative cross sections. A further argument against a vector pomeron is that it does not give any contribution to photoproduction data, as we show in [1]. One may also ask about the possibility of a scalar coupling of the pomeron to external particles. While possible from the point of view of quantum field theory, such a coupling is experimentally disfavored. In [6] it was shown that STAR data on polarized elastic pp scattering are compatible with the tensor pomeron but clearly rule out scalar pomeron couplings.

2. DIS in the tensor pomeron model

Good fits of some DIS data in the context of Regge theory have been obtained in the literature, see for example [4]. However, these do not explicitly treat the couplings of the pomeron (assumed to be a vector) to the photon and proton. In [1] we have addressed the question whether a Regge model based on the tensor pomeron, treating in full detail its tensor couplings to the photon and proton, can successfully describe DIS and photoproduction data. For making such a comparison to DIS data, we have added a hard pomeron to the model of soft high-energy reactions of [5]. The reggeon contribution, denoted by \mathbb{R}_+ , is dominated by the f_2 but can contain a small contribution from the a_2 . The parameters of the model are summarized in table 1. The indices $j = 0, 1, 2$ always refer to the hard pomeron, the soft pomeron, and the reggeon, respectively. The couplings of the pomerons and the reggeon to the photon contain functions \hat{a}_j and \hat{b}_j which we cannot derive from first principles. In fitting the data we make polynomial ansätze for them.

	hard pomeron \mathbb{P}_0	soft pomeron \mathbb{P}_1	reggeon \mathbb{R}_+
intercept	$\alpha_0(0) = 1 + \varepsilon_0$	$\alpha_1(0) = 1 + \varepsilon_1$	$\alpha_2(0) = 1 + \varepsilon_2$
slope parameter	α'_0	α'_1	α'_2
W^2 parameter	$\tilde{\alpha}'_0$	$\tilde{\alpha}'_1$	$\tilde{\alpha}'_2$
pp coupling parameter	β_{0pp}	β_{1pp}	β_{2pp}
$\gamma^*\gamma^*$ coupling functions	$\hat{a}_0(Q^2), \hat{b}_0(Q^2)$	$\hat{a}_1(Q^2), \hat{b}_1(Q^2)$	$\hat{a}_2(Q^2), \hat{b}_2(Q^2)$

Table 1: Parameters of our two-tensor-pomeron model.

We use the standard variables for DIS, namely the lepton-proton c. m. energy \sqrt{s} , the photon virtuality Q^2 , the c. m. energy W of the photon-proton system, Bjorken $x = Q^2/(W^2 + Q^2 - m_p^2)$, and $y = (W^2 + Q^2 - m_p^2)/(s - m_p^2)$. Then, the total cross sections σ_T and σ_L for transversely and longitudinally polarized photons resulting from our two-tensor-pomeron model are

$$\sigma_T(W^2, Q^2) = 4\pi\alpha_{\text{em}} \frac{W^2 - m_p^2}{W^2} \sum_{j=0,1,2} 3\beta_{jpp} (W^2 \tilde{\alpha}'_j)^{\varepsilon_j} \cos\left(\frac{\pi}{2} \varepsilon_j\right) \quad (2.1)$$

$$\times \left\{ \hat{b}_j(Q^2) \left[1 + \frac{2Q^2}{W^2 - m_p^2} + \frac{Q^2(Q^2 + 2m_p^2)}{(W^2 - m_p^2)^2} \right] - 2Q^2 \hat{a}_j(Q^2) \left[1 + \frac{2Q^2}{W^2 - m_p^2} + \frac{Q^2(Q^2 + m_p^2)}{(W^2 - m_p^2)^2} \right] \right\},$$

$$\sigma_L(W^2, Q^2) = 4\pi\alpha_{\text{em}} \frac{W^2 - m_p^2}{W^2} Q^2 \sum_{j=0,1,2} 3\beta_{jpp} (W^2 \tilde{\alpha}'_j)^{\varepsilon_j} \cos\left(\frac{\pi}{2} \varepsilon_j\right) \quad (2.2)$$

$$\times \left\{ 2\hat{a}_j(Q^2) \left[1 + \frac{2Q^2}{W^2 - m_p^2} + \frac{Q^2(Q^2 + m_p^2)}{(W^2 - m_p^2)^2} \right] + \hat{b}_j(Q^2) \frac{2m_p^2}{(W^2 - m_p^2)^2} \right\}.$$

They are related to the structure functions F_2 and F_L in the standard way,

$$F_2(W^2, Q^2) = \frac{Q^2}{4\pi^2\alpha_{\text{em}}} (1-x) [1 + 2\delta(W^2, Q^2)]^{-1} [\sigma_T(W^2, Q^2) + \sigma_L(W^2, Q^2)] \quad (2.3)$$

$$F_L(W^2, Q^2) = \frac{Q^2}{4\pi^2\alpha_{\text{em}}} (1-x) \sigma_L(W^2, Q^2) \quad (2.4)$$

with $\delta(W^2, Q^2) = 2m_p^2 Q^2 / (W^2 + Q^2 - m_p^2)^2$. We use standard values for the electromagnetic coupling α_{em} and the proton mass m_p .

3. Fit to DIS and photoproduction

Using our model we perform a fit to the available DIS [7] and photoproduction data [8, 9, 10, 11] in the kinematic range given by $6 < \sqrt{s} < 318$ GeV, $Q^2 < 50$ GeV², and $x < 0.01$. We fit the reduced cross section

$$\sigma_{\text{red}}(W^2, Q^2, y) = \frac{1 + (1-y)^2 + y^2 \delta(W^2, Q^2)}{1 + (1-y)^2} \left[F_2(W^2, Q^2) - \frac{\tilde{f}(W^2, Q^2, y) F_L(W^2, Q^2)}{1 + 2\delta(W^2, Q^2)} \right], \quad (3.1)$$

where

$$\tilde{f}(W^2, Q^2, y) = \frac{y^2 [1 + 2\delta(W^2, Q^2)]}{1 + (1-y)^2 + y^2 \delta(W^2, Q^2)}. \quad (3.2)$$

It contains the full experimental information and is the quantity that is actually measured. Some of the couplings and slope parameters in our model are well constrained from other experiments so that we use their known values as default parameters.

Formally, our fit has 25 parameters. However, not all of them are equally important. The most important parameters are the intercepts of the pomerons and of the reggeon. Further parameters of significance are the values of the coupling functions $\hat{a}_j(Q^2)$ and $\hat{b}_j(Q^2)$ at $Q^2 = 0$. The remaining parameters are used to describe the fall-off of the coupling functions \hat{a}_j and \hat{b}_j at large Q^2 , and these 17 parameters are much less significant for our result. The fit is of very satisfactory quality, for a detailed quantification of the fit quality see [1]. For the intercepts of the hard pomeron, the soft pomeron, and the reggeon we find, respectively,

$$\alpha_0(0) = 1.3008 \left({}^{+73}_{-84} \right), \quad \alpha_1(0) = 1.0935 \left({}^{+76}_{-64} \right), \quad \alpha_2(0) = 0.485 \left({}^{+88}_{-90} \right). \quad (3.3)$$

Figure 1 shows a comparison of our tensor-pomeron fit to the photoproduction cross sections of [8, 9, 10, 11]. We find that photoproduction is dominated by the soft pomeron, while the hard

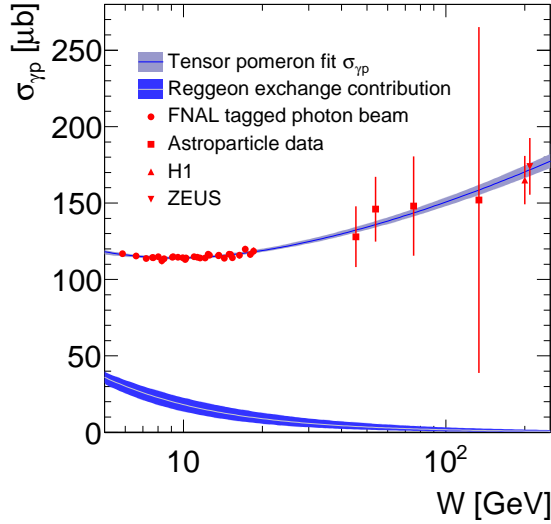


Figure 1: Comparison of our fit to the photoproduction cross sections [8, 9, 10, 11], with the reggeon contribution also shown separately. The experimental uncertainties of the fit are indicated as shaded bands.

pomeron contribution is compatible with zero here. As an example, we quote the three different contributions for $W = 200$ GeV:

$$\begin{aligned} 170.4^{+4.2}_{-4.0} \mu\text{b} & \quad \text{for the soft pomeron } \mathbb{P}_1, \\ 0.002^{+0.086}_{-0.002} \mu\text{b} & \quad \text{for the hard pomeron } \mathbb{P}_0, \\ 0.84^{+0.99}_{-0.58} \mu\text{b} & \quad \text{for the } \mathbb{R}_+ \text{ reggeon.} \end{aligned}$$

The reggeon contribution, also shown in the figure, is sizable for low W . We point out again that a vector pomeron would give zero contribution to the photoproduction cross section.

Next, we turn to DIS. Figure 2 compares of our fit results, shown as a blue band, to the DIS cross sections of [7]. Here we have chosen as an example the data for $\sqrt{s} = 318$ GeV and low

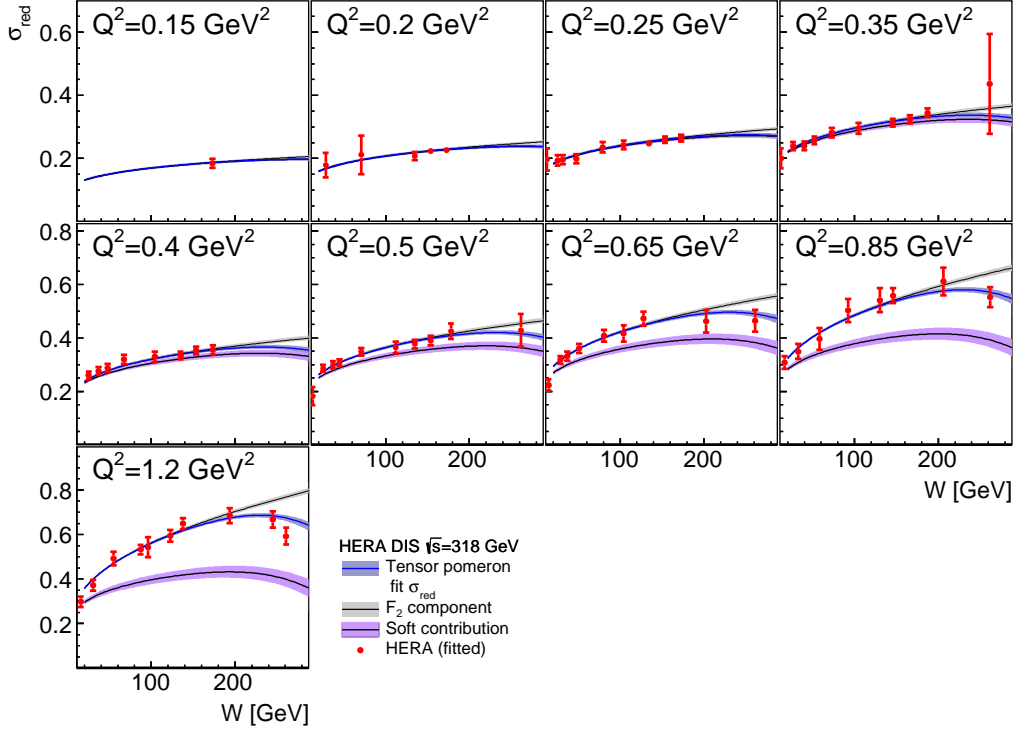


Figure 2: Comparison of our fit to DIS cross sections [7] at $\sqrt{s} = 318$ GeV, at low $Q^2 < 1.5$ GeV². We also show the soft contribution (soft pomeron plus \mathbb{R}_+ reggeon) and the contribution of the structure function F_2 in the reduced cross section. The experimental uncertainties of the fit are indicated as shaded bands.

$Q^2 < 1.5$ GeV². We indicate the soft contribution (soft pomeron plus reggeon) as a purple band in figure 2. The thin grey band represents the contribution of the structure function F_2 to the reduced cross section, cf. equation (3.1).

The fit is of similarly good quality as in figure 2 for the whole kinematic range that we consider. In the full kinematic range we find the following properties. The hard contribution increases with increasing Q^2 , and the hard and soft contributions are of approximately equal size at $Q^2 = 5$ GeV². But the soft contribution is still visible at $Q^2 = 20$ GeV². The difference between σ_{red} and F_2 , due to the longitudinal cross section σ_L , is clearly visible at large W . As expected, the reggeon contribution becomes very small at large W .

We have also computed the ratio $R = \sigma_L/\sigma_T$ from our fit results for the longitudinal and transverse cross sections. We compare this to the R data from H1 [12] which are extracted directly from cross section measurements at fixed Q^2 but different c.m. energies. We observe that our fit prefers higher values for R . The origin of this discrepancy and its significance in view of the sizable error of the R data from H1 are difficult to assess. Measurements of σ_L and of R at a future electron-ion collider would be very helpful to improve our understanding of the dynamics of the longitudinal cross section.

4. Summary

We have developed a two-tensor-pomeron model and have made a fit to photoproduction data and to small- x DIS data from HERA. We obtain a very satisfactory fit and determine in particular the intercepts of the two pomerons. For DIS, the soft contribution is still clearly visible up to about $Q^2 = 20 \text{ GeV}^2$. The transition from low to high Q^2 is nicely described.

We have argued that a vector pomeron, that is a pomeron with vector type couplings, is excluded by general arguments based on quantum field theory. For instance, it would not give any contribution to photoproduction in clear contradiction with the data. A tensor pomeron, on the other hand, is compatible with quantum field theory and permits an excellent description of photoproduction and DIS data, as we have shown.

References

- [1] D. Britzger, C. Ewerz, S. Glazov, O. Nachtmann and S. Schmitt, *The Tensor Pomeron and Low- x Deep Inelastic Scattering*, arXiv:1901.08524 [hep-ph].
- [2] O. Nachtmann, *Considerations concerning diffraction scattering in quantum chromodynamics*, Annals Phys. **209** (1991) 436.
- [3] A. Donnachie and P. V. Landshoff, *pp and $\bar{p}p$ Elastic Scattering*, Nucl. Phys. B **231** (1984) 189.
- [4] A. Donnachie and P. V. Landshoff, *Small x : Two pomerons!*, Phys. Lett. B **437** (1998) 408 [hep-ph/9806344].
- [5] C. Ewerz, M. Maniatis and O. Nachtmann, *A Model for Soft High-Energy Scattering: Tensor Pomeron and Vector Odderon*, Annals Phys. **342** (2014) 31 [arXiv:1309.3478 [hep-ph]].
- [6] C. Ewerz, P. Lebiedowicz, O. Nachtmann and A. Szczurek, *Helicity in proton-proton elastic scattering and the spin structure of the pomeron*, Phys. Lett. B **763** (2016) 382 [arXiv:1606.08067 [hep-ph]].
- [7] H. Abramowicz *et al.* [H1 and ZEUS Collaborations], *Combination of measurements of inclusive deep inelastic $e^\pm p$ scattering cross sections and QCD analysis of HERA data*, Eur. Phys. J. C **75** (2015) no.12, 580 [arXiv:1506.06042 [hep-ex]].
- [8] S. Aid *et al.* [H1 Collaboration], *Measurement of the total photon-proton cross-section and its decomposition at 200 GeV center-of-mass energy*, Z. Phys. C **69** (1995) 27 [hep-ex/9509001].
- [9] S. Chekanov *et al.* [ZEUS Collaboration], *Measurement of the photon-proton total cross-section at a center-of-mass energy of 209 GeV at HERA*, Nucl. Phys. B **627** (2002) 3 [hep-ex/0202034].
- [10] G. M. Vereshkov, O. D. Lalakulich, Y. F. Novoseltsev and R. V. Novoseltseva, *Total cross section for photon-nucleon interaction in the energy range $\sqrt{s} = 40 \text{ GeV} - 250 \text{ GeV}$* , Phys. Atom. Nucl. **66** (2003) 565 [Yad. Fiz. **66** (2003) 591].
- [11] D. O. Caldwell *et al.*, *Measurements of the Photon Total Cross-Section on Protons from 18 GeV to 185 GeV*, Phys. Rev. Lett. **40** (1978) 1222.
- [12] V. Andreev *et al.* [H1 Collaboration], *Measurement of inclusive ep cross sections at high Q^2 at $\sqrt{s} = 225$ and 252 GeV and of the longitudinal proton structure function F_L at HERA*, Eur. Phys. J. C **74** (2014) 2814 [arXiv:1312.4821 [hep-ex]].